REVIEW OF EXPERIMENTS ON THE WISCONSIN TOKAMAK

PLP 754 JUNE 1978

J. C. Sprott
R. J. Groebner
D. J. Holly
A. P. Biddle
B. Lipschultz

Plasma Studies *University of Wisconsin-Madison*

On December 9, 1977, after 14 years of operation, the small toroidal octupole was converted into a tokamak by removing the remaining two hoops. (The first two hoops had been removed six weeks earlier. See PLP 740.) The device was operated as a tokamak for nine weeks until February 10, 1978, when it was dismantled to make room for the Tokapole II device. This report summarizes the experimental results obtained during the tokamak phase of operation.

As a tokamak, the machine parameters are as follows:

Major radius: 43.18 cm

Minor cross section: 35.56 × 35.56 cm square

Toroid walls: aluminum, 1.905 cm thick with poloidal and toroidal insulated gaps

Vacuum volume: 300 liters

B_T on axis: 3 kG (typical), 6 kG (maximum)

L/R time of B_T: 2 msec

Available OH voltage: 83 volts

Poloidal flux: 0.1 weber

Available energy (poloidal + toroidal fields): 162 kJ

(54 - 240 μF, 5 kV capacitors)

Base vacuum: 2×10^{-7} torr

Preionization: 50 W, 2.45 GHz; 10 kW, 9 GHz

DC vertical field: 0-30 gauss (either polarity)

The first experiment was to measure the toroidal current as a function of the single turn ohmic heating voltage with all parameters adjusted in the way that optimized the plasma current in the Tokapole configuration. It was necessary to puff H_2 gas to a pressure about 2-3 times higher than in the tokapole (i.e., $p_0 \sim 5 \times 10^{-4}$ torr, true). The toroidal current was determined by measuring the primary

OH current and multiplying by the turns ratio (60) after verifying that the current is negligibly small in the absence of a plasma. The current vs. voltage is shown in figure 1, along with the same quantities for the two tokapole configurations. Unlike the tokapole, the tokamak has a nearly constant plasma resistance. The peak current is higher for the tokamak (∿50 kA), but that is because a higher OH voltage is available in the tokamak. The scaling is more favorable in the tokapole, however. If the current is assumed to flow uniformly over the square cross section of the tokamak, the resistivity temperature (for $Z_{eff} = 1$) is 6 eV. At the highest OH voltage, the input power is 3 megawatts (60 V × 50 kA). These measurements were made without a vertical field, relying on the conducting wall to provide the plasma equilibrium.

Spectroscopic observations of vacuum ultraviolet (VUV) radiation from the tokamak discharges were made with a 1-meter Seya-Namioka monochromator and with a 1/2-meter Seya. The 1/2-meter instrument had no exit slit so that a large number of spectral lines could be observed during one discharge. Photons were detected by a microchannel plate, and its output was a set of lines on a phosphorescent screen which were visible to the human eye and could be photographed.

Typical output from the ½-meter Seya is exhibited in figure 2. For this shot, the poloidal and toroidal banks were charged to 2.5 kV. On one shot, lines in the range 600-1350 Å are observed, and this technique is a powerful means to determine what effect altering various discharge parameters will have on the VUV radiation.

Observations with both instruments indicated that OI, OII, OIII, OIV, CI, CII, CIII, CIV NI, NII, NIII, and NIV were present in the hydrogen discharges. (The nitrogen lines were bright only when there was a significant air leak in the vacuum system.) The lines of the higher ionization states were not observed in low power

discharges. On occasion, some aluminum lines were also seen, and a fluorine line was present when a piece of teflon was inadvertently exposed to the plasma.

Figures 3-6 show the time history of the intensity of the brightest lines of CI, CII, CIII, and CIV, respectively. In each figure, the upper picture has a time scale of 0.2 ms/div while the lower picture has a time scale of 0.1 ms/div. The pictures with the higher time resolution show that the ionization states appear in succession, as one would expect. Also light from each ion has an initial peak. This is interpreted as the ionization peak for the given ion. The ionization peak occurs during rapid ionization of an ion to the next higher ionization state and normally the light would be expected to drop quickly to a low level after the occurrence of this peak. However, in these discharges the light output of all the ions rose after their ionization peaks, and this strongly suggests that there was a continuous influx of carbon into the plasma. This is consistent with other observations; in particular, measurements of the current density with a Rogowski loop showed that the current channel was leaning on the outer wall of the toroid, and thus one might expect a strong plasma-wall interaction which would inject impurities into the discharge.

The pictures show that light output from CI and CII was relatively constant during the discharge (at least, up to 2 ms after the initiation of the discharge.) This suggests that there was a relatively constant flow of fresh carbon into the plasma. In contrast, the CIII and CIV lines both peak at about 800 μs and then decay with the CIV light decaying faster than the CIII light. The simplest explanation of these data is that the electron temperature peaked at about 800 μs and then started to drop. Thus fresh CIII and CIV could not be produced fast enough to replace the ions which escaped from the plasma. (The poloidal and toroidal banks were charged to 3.0 kV for these discharges.)

For a standard tokamak discharge, the conductivity temperature was about 8 eV. Much effort was expended to determine T_e from spectroscopic data. This was not an easy task since the plasma in a tokamak discharge is neither in complete thermal equilibrium nor in local thermal equilibrium. Thus, the populations of the excited states of an ion do not follow the Boltzmann relationship. To calculate these populations, one must know the excitation rate coefficients to the desired levels as a function of T_e. In general, the atomic data needed are poorly known, if they exist at all, although for the resonance transitions from the ground states the data are fairly good now. Unfortunately, we were not in a position to use the good data.

However, by several crude techniques we arrived at a T_e estimate of 10-20 eV. One such estimate came from the fact that several CIV lines, originating from energy levels about 50 eV above the ground state, were not observed. Excitations from the ground state to these excited levels were expected to have been strong if T_e was 30 eV or more. The fact that the lines were not observed at all strongly suggests that T_e was not more than 20 or 25 eV at most.

One measurement was made of the Doppler broadening of the H_β line. The line width observed was consistent with a hydrogen atom temperature of 5 eV. One thus expects that T_i had a lower limit of 5 eV. However, this measurement was made only once and should be interpreted cautiously.

Often interesting fluctuations were observed in various plasma parameters. No definite source for the fluctuations was determined, but some observations are presented for their own sake. Figure 7 shows the plasma current and single turn voltage traces for a particular discharge. (The upper trace is voltage and the lower trace is current. The camera reflected these traces about a horizontal axis.)

Note the 3 large spikes and the smaller ripples occurring simultaneously in the current and voltage. Figures 8 and 9 are respectively the L_α and $\dot{B}$ traces from the same discharge. (The oscillograms have a time scale of 0.2 ms/div.) The $\dot{B}$ trace has large spikes at 550 μs, 1000 μs, and 1320 μs. There coincided exactly with the big spikes in current and voltage. It can also be seen that the L_α light jumps up at each of these times. Figure 10 shows simultaneous traces of L_α and the plasma current for another discharge. The same type of behavior was present.

These observations suggest that oscillations occurred in the current channel so that plasma was thrown into the wall, and that fresh gas was released to enter the discharge to be excited and ionized.

A Langmuir probe biased to -45 V was used to scan the ion saturation current j_{sat} in the midplane, in both the vertical and horizontal directions. The vertical scan is shown in Fig. 11 and Fig. 12 and the horizontal scan in Fig. 13. A 40 GHz interferometer was mounted in the machine with the horns at the top and bottom midplane. For $n_e \lesssim 2 \times 10^{12}$ cm^{-3} the interferometer fringe shifts gave an electron density value consistent with the Langmuir probe measurements, assuming a T_e around 10 eV; for densities higher than this the amplitude of the transmitted microwave signal was essentially zero.

Initial work for first the detection and then the measurement of fast magnetosonic eigenmodes in the tokamak configuration was performed in anticipation of the Tokapole II device. The blanked-off hoop supports provided ideal mounts for the coupling structures. Identical 3/8" brass rods were installed in two outer supports 120° apart. These rods extended vertically through the machine, and had glass insulating sleeves. They were used as either receiving or transmitting structures. The RF source consisted of a 20-watt amateur transmitter operating

at either 7 or 14 MHz, a linear amplifier that could be driven to 200 watts, and a matching device capable of transforming a wide range of reactances to 50 ohms. The launching structures were driven in a low-inductance balanced mode to maximize the current in the antenna.

The received signal was taken off a similar antenna using a balanced transformer and a 250 kHz parrband filter. Initial measurements were indeterminate as the signal-to-noise ratio was too high. Both antennas were moved to the inner support positions with the intent of minimizing the parasitic loading. The slightly reduced density surrounding the antennae allowed good reception of the transmitted signals, though the transmitted signal was still heavily attenuated. The eigenmodes appeared as sharp peaks above the background signal. A final test was made by adjusting the toroidal field so as to bring ω_{ci} into the chamber. As expected, the heavy fundamental absorption damped the fast magnetosonic wave.

While such complications as the strong poloidal magnetic field around the hoops as well as the somewhat more constricted current channel in Tokapole II are expected to introduce further complications, the tokamak experiment gives good hope of being able to perform fast wave heating in the new machine.

Because the eigenmodes in such a small machine are widely spaced as a function of density, the rapid density fluctuations made it impossible to match to the eigenmodes themselves. Rather, multiple shots were taken while monitoring the reflected power as seen between the matching network and the transmitter. The general plasma loading, called "parasitic loading" was matched. However, small increases in reflected power corresponding to changes in the plasma density as measured by the line average probe were noted. There peaks were in the direction indicating an increased load, which is commensurate with eigenmodes. The density of modes increased markedly when going from 7 to 14 MHz, as would be expected.

CURRENT PROFILE:

Using a rogowski type current probe, we were able to find the current profile as a function of space and time. The current starts up pretty uniformly over the square cross section, peaking slightly ∿3" inside the major radius of the machine. The peak current then, with no vertical field stabilization, moves outward increasing its major radius (See figures 14-19). By 2.5 ms the current is resting against the outer wall. The image currents in the wall provide a vertical field which keeps the current from going any further. We wound our own vertical field but found that the vertical field generated was too small by a factor of 5 to keep the current centered at peak. Also, because we had to use a D.C. vertical field meant for peak current, the plasma would be harder to start up. At lower currents the plasma would be pushed into the inner wall. In effect, if one cannot program the vertical field, it is better to use the walls instead for horizontal stabilization of the current channel.

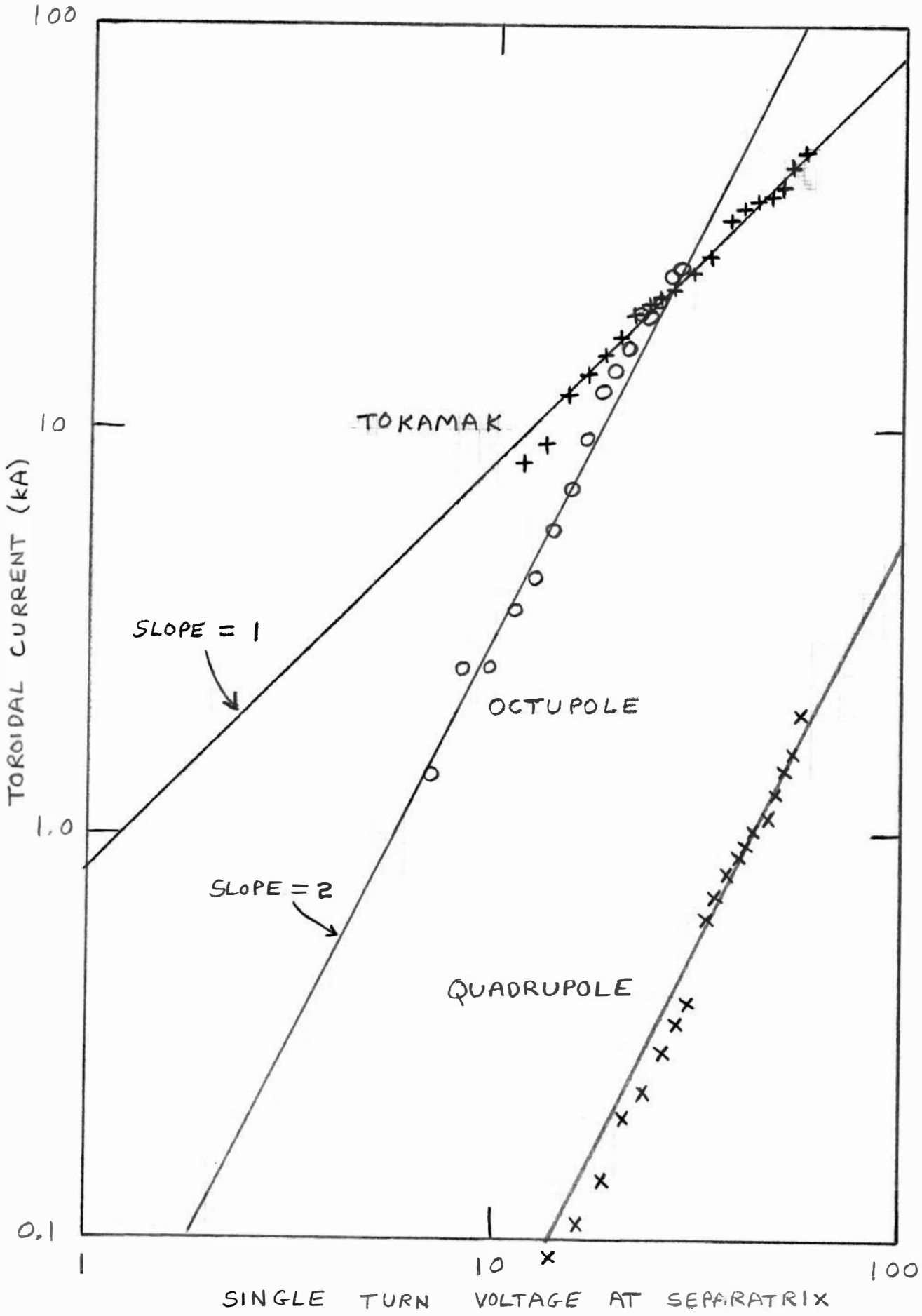
100
10
1.0
0.1
TOROIDAL CURRENT (kA)
TOKAMAK
SLOPE = 1
OCTUPOLE
SLOPE = 2
QUADRUPOLE
1
10
100
SINGLE TURN VOLTAGE AT SEPARATRIX

FIG 1

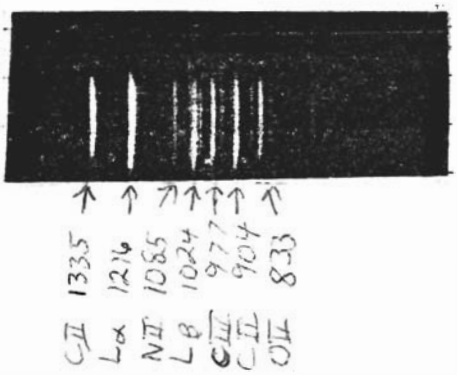

FIG. 2

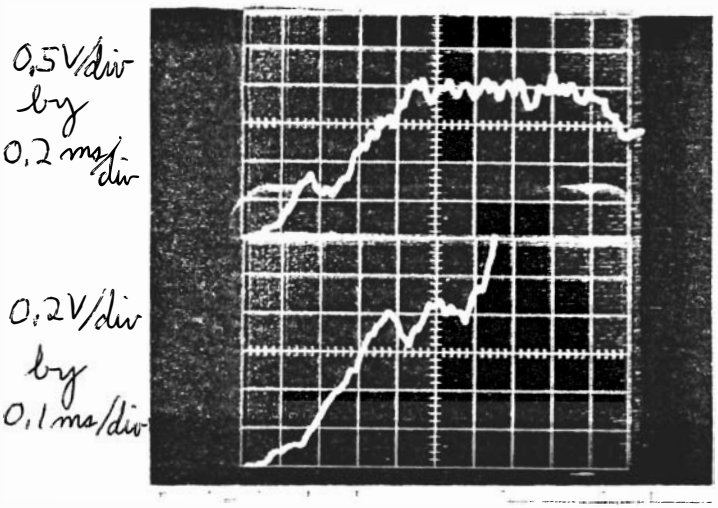

FIG. 3 (CI 1561)

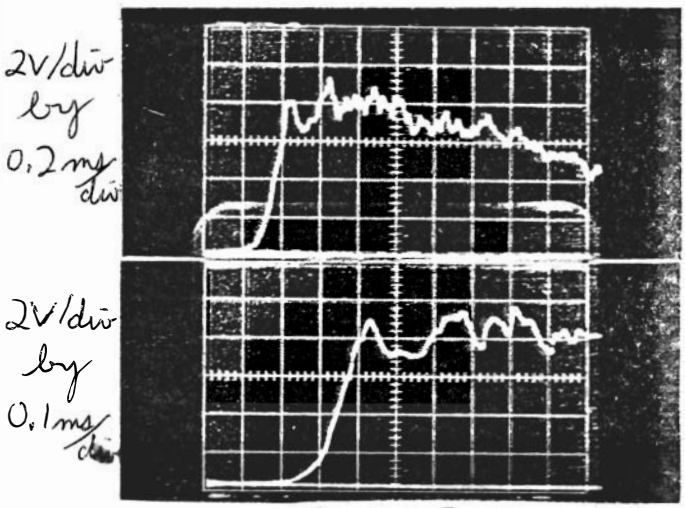

FIG. 4 (CII 1335)

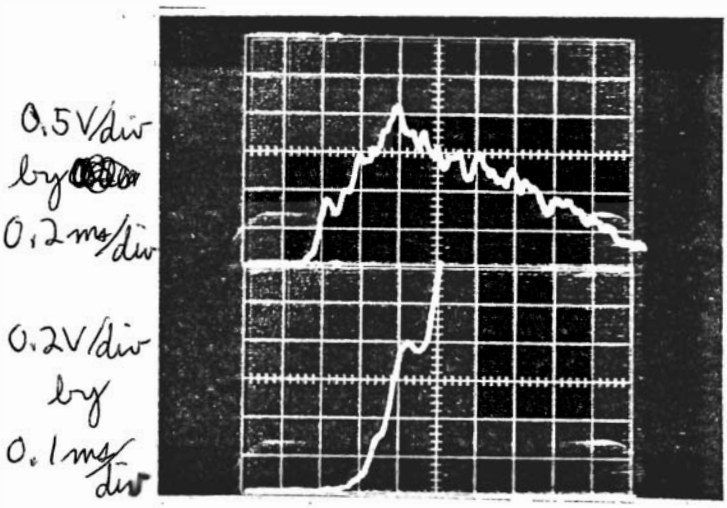

FIG. 5 (CIII 977)

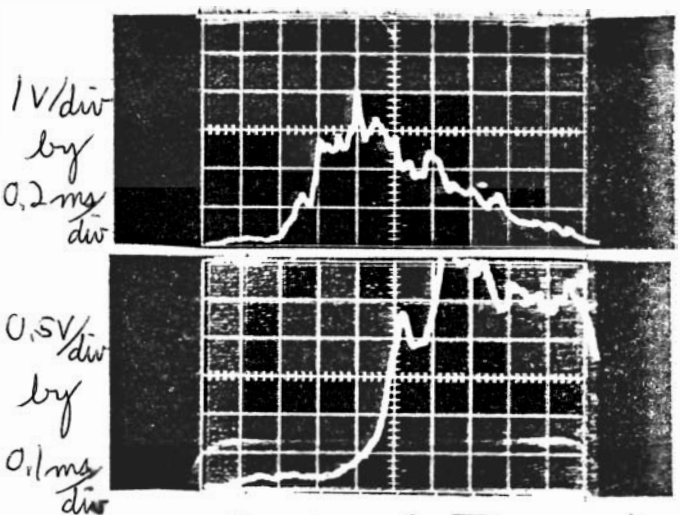

FIG. 6 (CIV 1549)

Upper Trace is Loop Voltage. Lower Trace is I_p.

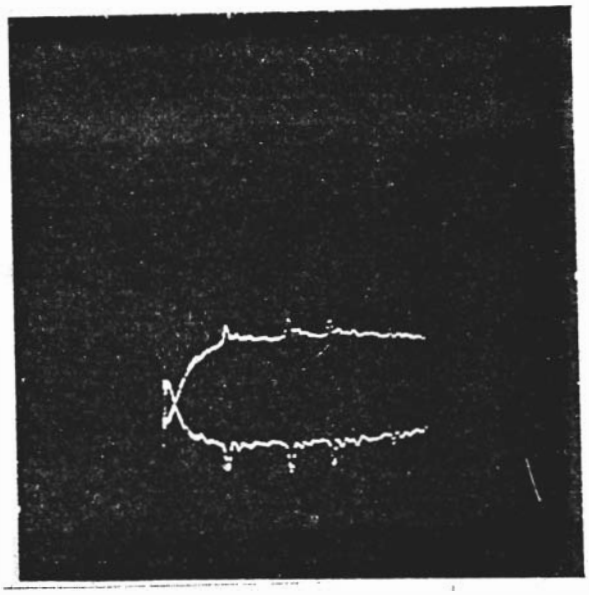

FIG. 7 (2 ms full scale)

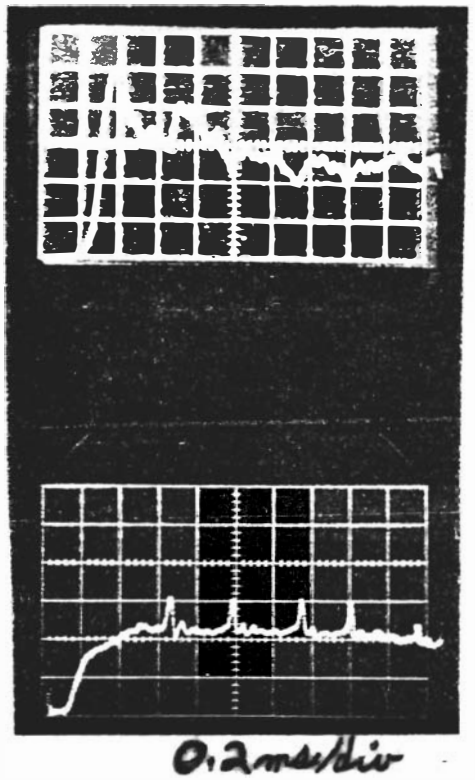

FIG. 10

L_2

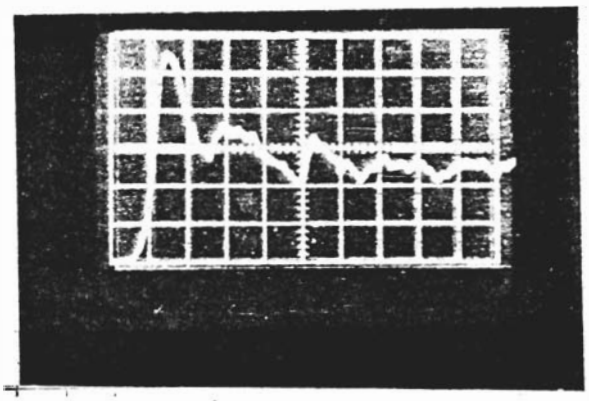

FIG. 8 (0.2 ms/div)

$\dot{B}$

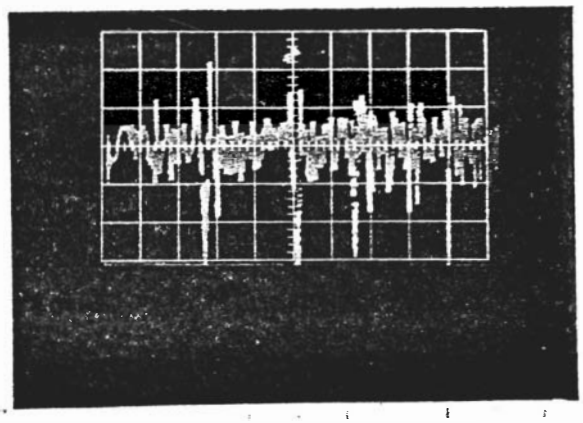

FIG. 9 (0.2 ms/div)

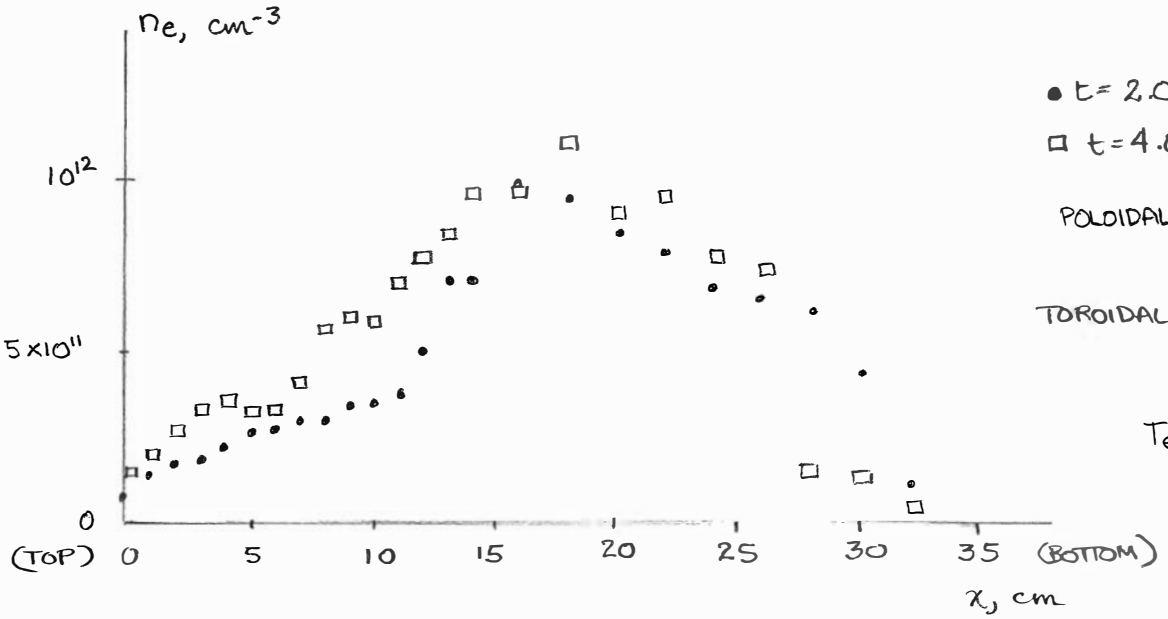
n_e, cm^{-3}
10^{12}
5×10^{11}
0
(TOP) 0 5 10 15 20 25 30 35 (BOTTOM)
x, cm
• t = 2.0 msec
□ t = 4.0 msec
POLOIDAL BANK VOLTAGE = 1.0 kV
TOROIDAL BANK VOLTAGE = 2.0 kV
T_e ASSUMED 10eV

FIG. 11

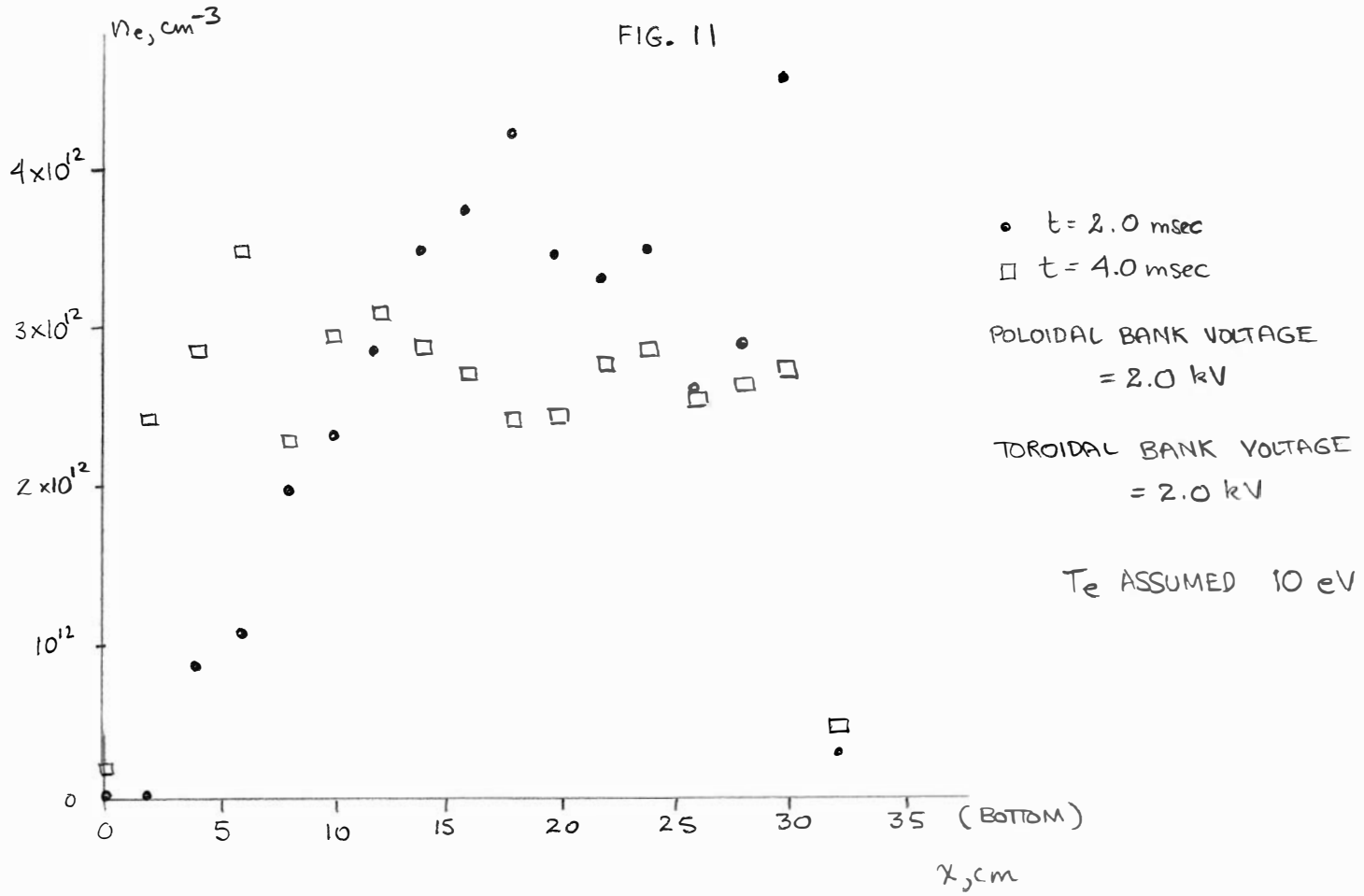
n_e, cm^{-3}
4×10^{12}
3×10^{12}
2×10^{12}
10^{12}
0
0 5 10 15 20 25 30 35 (BOTTOM)
x, cm
• t = 2.0 msec
□ t = 4.0 msec
POLOIDAL BANK VOLTAGE = 2.0 kV
TOROIDAL BANK VOLTAGE = 2.0 kV
T_e ASSUMED 10 eV

FIG. 12

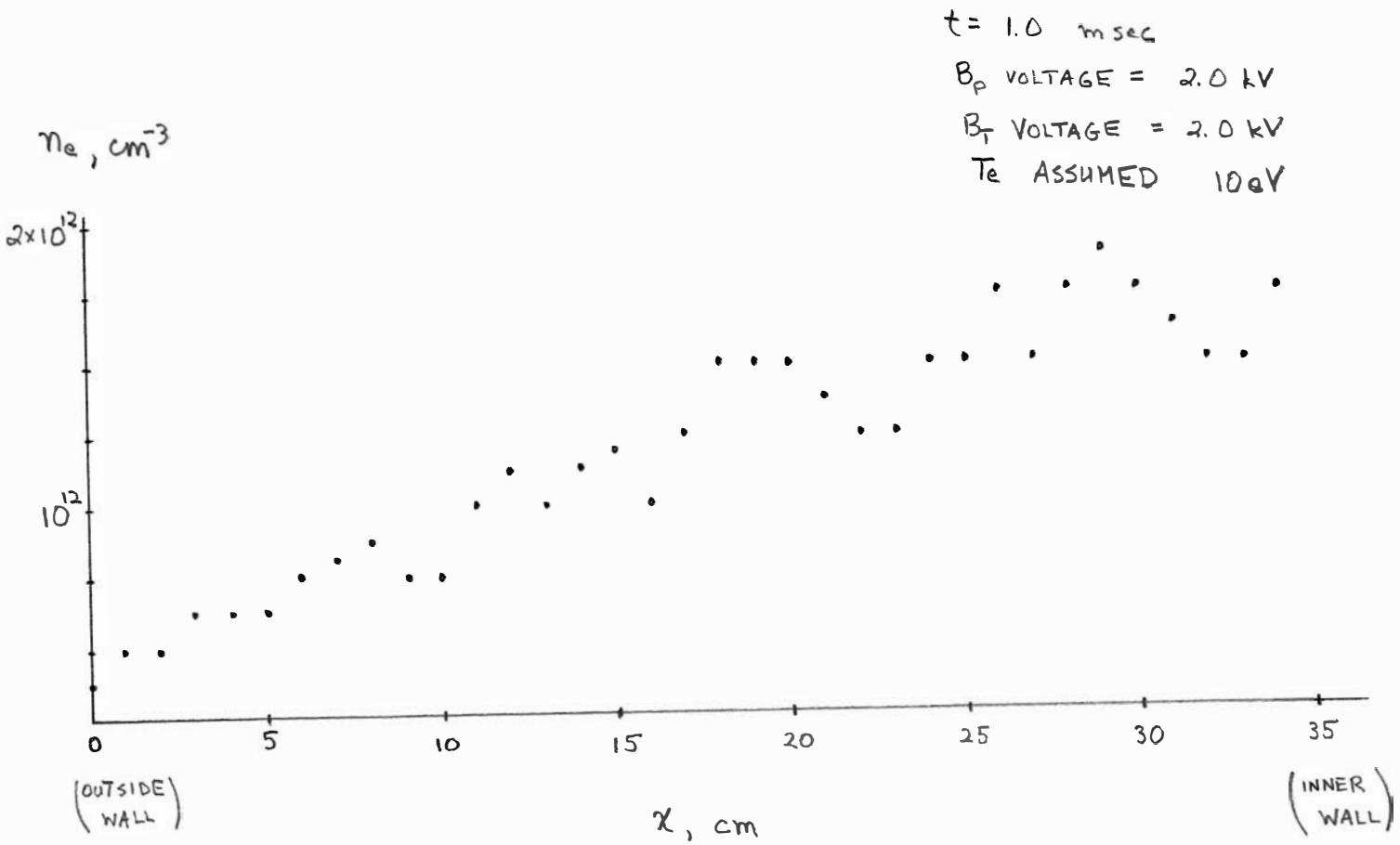
t = 1.0 m sec
B_p VOLTAGE = 2.0 kV
B_T VOLTAGE = 2.0 kV
Te ASSUMED 10eV
n_e, cm^{-3}
2×10^{12}
10^{12}
0
5
10
15
20
25
30
35
(OUTSIDE WALL)
(INNER WALL)
x, cm

FIG. 13

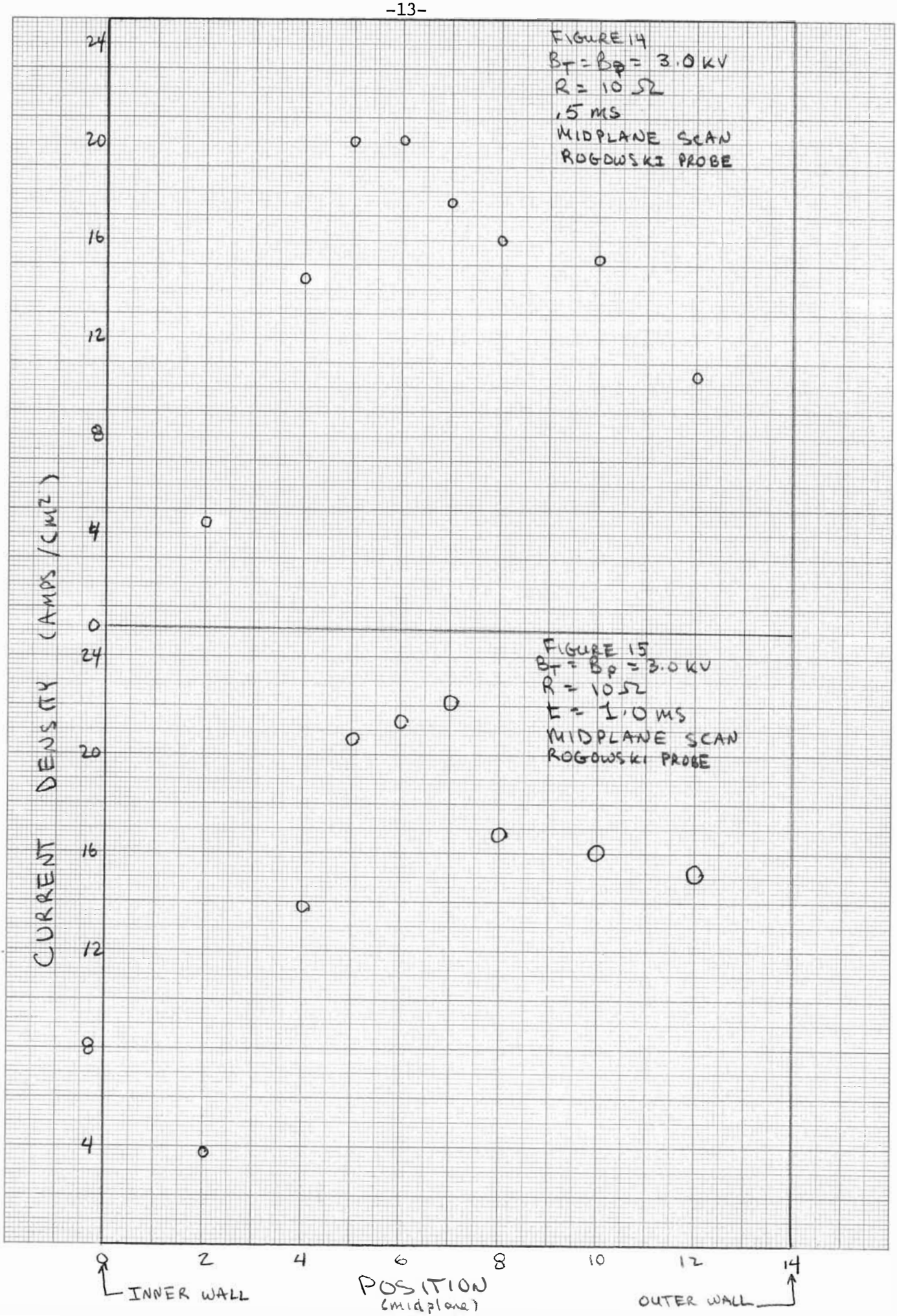

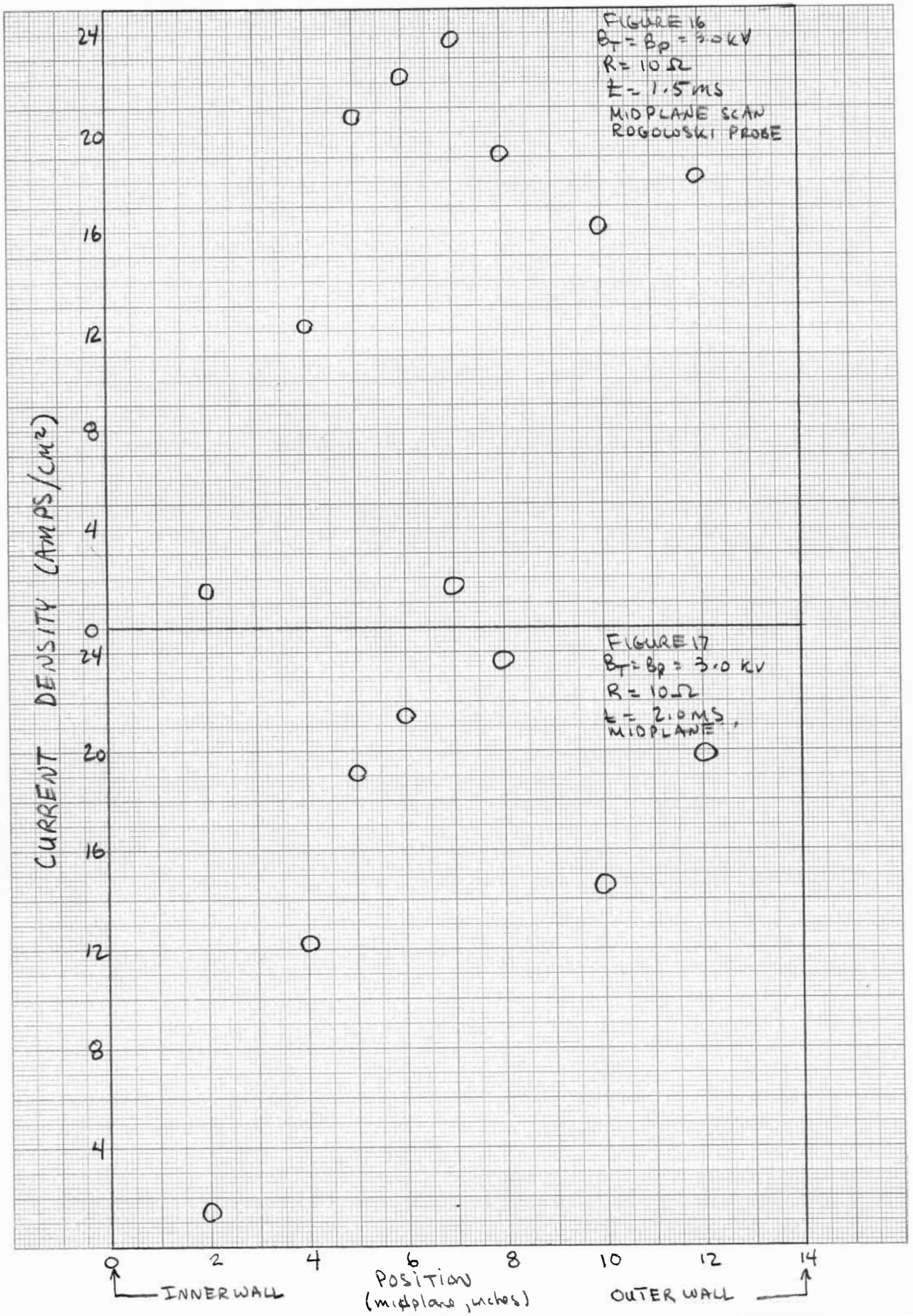
FIGURE 16
$B_T = B_p = 3.0$ KV
R = 10 Ω
t = 1.5 MS
MIDPLANE SCAN
ROGOWSKI PROBE
FIGURE 17
$B_T = B_p = 3.0$ KV
R = 10 Ω
t = 2.0 MS,
MIDPLANE
CURRENT DENSITY (AMPS/CM²)
0
4
8
12
16
20
24
0
2
4
6
8
10
12
14
INNER WALL
POSITION
(midplane, inches)
OUTER WALL